IOPscience iopscience.iop.org

Home Search Collections Journals About Contact us My IOPscience

Damped Bloch oscillations of Bose–Einstein condensates in disordered potential gradients

This content has been downloaded from IOPscience. Please scroll down to see the full text.

2008 New J. Phys. 10 045027

(http://iopscience.iop.org/1367-2630/10/4/045027)

View the table of contents for this issue, or go to the journal homepage for more

Download details:

IP Address: 194.95.157.145
This content was downloaded on 06/04/2017 at 08:45

Please note that terms and conditions apply.

You may also be interested in:

Superfluid dynamics of a Bose–Einstein condensate in a periodic potential
C Menotti, A Smerzi and A Trombettoni

Superfluid Bloch dynamics in an incommensurate optical lattice
J B Reeves, B Gadway, T Bergeman et al.

Analysis of localization phenomena in weakly interacting disordered lattice gases
T Schulte, S Drenkelforth, J Kruse et al.

Localization and anomalous transport in a 1D soft boson optical lattice
A K Tuchman, W Li, H Chien et al.

Coherent transport of BECs in lattices
M L Chiofalo and M P Tosi

The physics of dipolar bosonic quantum gases
T Lahaye, C Menotti, L Santos et al.

Resonant tunneling of Bose–Einstein condensates in optical lattices
Alessandro Zenesini, Carlo Sias, Hans Lignier et al.

Dynamics of Bloch oscillations
T Hartmann, F Keck, H J Korsch et al.

Atomic motion in tilted optical lattices: an analytical approach
Quentin Thommen, Jean Claude Garreau and Véronique Zehnlé

New Journal of Physics
The open-access journal for physics

Damped Bloch oscillations of Bose–Einstein condensates in disordered potential gradients

S Drenkelforth[1,3], G Kleine Büning[1], J Will[1], T Schulte[1], N Murray[1], W Ertmer[1], L Santos[2] and J J Arlt[1]

[1] Institut für Quantenoptik, Leibniz Universität Hannover, Welfengarten 1, D-30167 Hannover, Germany
[2] Institut für Theoretische Physik, Leibniz Universität Hannover, Appelstraße 2, D-30167 Hannover, Germany
E-mail: drenkelforth@iqo.uni-hannover.de

New Journal of Physics **10** (2008) 045027 (13pp)
Received 21 December 2007
Published 30 April 2008
Online at http://www.njp.org/
doi:10.1088/1367-2630/10/4/045027

Abstract. We investigate both experimentally and theoretically disorder-induced damping of Bloch oscillations of Bose–Einstein condensates in optical lattices. The spatially inhomogeneous force responsible for the damping is realized by a combination of a disordered optical and a magnetic gradient potential. We show that the inhomogeneity of this force results in a broadening of the quasimomentum spectrum, which in turn causes damping of the centre-of-mass oscillation. We quantitatively compare the obtained damping rates to the simulations using the Gross–Pitaevskii equation. Our results are relevant for high precision experiments on very small forces, which require the observation of a large number of oscillation cycles.

[3] Author to whom any correspondence should be addressed.

1367-2630/08/045027+13$30.00
© IOP Publishing Ltd and Deutsche Physikalische Gesellschaft

Contents

1. Introduction 2
2. Bloch oscillations in periodic potentials 3
3. Experimental realization 4
4. Damped Bloch oscillations 5
5. Conclusion 11
Acknowledgments 12
References 12

1. Introduction

The ability to realize ultracold quantum gases in periodic and disordered potentials has enabled detailed studies of fascinating effects originating in solid state physics. Ongoing investigations of single particle phenomena such as Anderson localization as well as many particle effects like the Bose–Glass phase and the Mott insulator [1]–[6] show the variety of possibilities these ensembles offer. Especially the non-intuitive dynamics of quantum gases in periodic potentials is of interest for theoretical and experimental investigations, since quantum gases have enabled the first direct observation of Bloch oscillations [7] in tilted periodic potentials [8]–[10]. In these systems, the periodicity leads to an oscillatory motion instead of a linear acceleration of the particles subjected to an external force.

In solid state systems scattering at imperfections of the crystal structure leads to damping of Bloch oscillations on timescales much shorter than the oscillation period itself. Therefore Bloch oscillations of electrons are only observable in semiconductor superlattices [11], where the large spatial period leads to high oscillation frequencies, which are faster than the damping. Optical lattices on the other hand constitute perfect optical crystals and allow for the observation of long-lived Bloch oscillations [12]–[15]. The experimental control of lattice parameters such as lattice depth and spacing, the possibility to detect the atomic cloud with absorption imaging and the very small momentum spread of Bose–Einstein condensates (BECs) have enabled detailed studies of this quantum effect.

A comparison of these systems gives rise to the question: How will the controlled addition of disorder to an optical lattice affect the dynamics of particles in such a periodic potential? Disorder can be realized with additional optical potentials [2, 5], [16]–[21], [36], impurity atoms [22, 23] or the roughness of the trapping potential close to the surface of atom chips [24]. The simultaneous application of a homogeneous force and the optical disorder potential constitutes a spatially inhomogeneous acceleration. This inhomogeneity can have important consequences for the application of Bloch oscillations as a sensitive tool for high precision measurements of small forces [12]–[14] [25, 26], since it leads to a dephasing of the quasimomentum and thus to a damping of the centre-of-mass oscillation [27]. Therefore a detailed quantitative understanding of the effect of the disorder and the underlying mechanism is indispensable for future applications.

We investigate the effect of a small disordered potential on Bloch oscillations of BECs in a one-dimensional (1D) optical lattice potential. Our results indeed show that the inhomogeneity leads to significant damping of the centre-of-mass motion. The damping rate increases with

disorder depth and is quantitatively compared to numerical simulations using the Gross–Pitaevskii equation (GPE). Furthermore, we show that the disorder-induced broadening of the quasimomentum distribution, which is the underlying mechanism for the damping of Bloch oscillations, reduces the fraction of atoms in the BEC.

2. Bloch oscillations in periodic potentials

The acceleration of particles in periodic potentials leads to an oscillatory motion instead of a linear increase in velocity. Since this is a pure single particle effect, it is possible to describe the underlying physics in a 1D model, while a quantitative analysis of the effects of disorder and interactions requires a 3D description, as reported in a previous work [27]. We briefly discuss the main features necessary for the understanding of Bloch oscillations while a comprehensive review can be found in [28].

The periodicity of the potential implies that the eigenfunctions obey the same translational symmetry as the potential

$$\phi(z+d) = \mathrm{e}^{\mathrm{i}qd}\phi(z), \tag{1}$$

where the phase difference q from site-to-site is called quasimomentum and d is the lattice constant. Since the eigenfunctions are periodic, it is possible to restrict the description of the dynamics to the first Brillouin zone $\left[-\frac{\pi}{d}, \frac{\pi}{d}\right]$. According to the acceleration theorem $q(t) = q_0(0) + \frac{F}{\hbar}t$ an additional potential gradient will cause the quasimomentum to evolve linearly in time, because the energy offset from site-to-site leads to a linear increase of the phase difference from site-to-site during the time evolution. In combination with the periodicity of the band structure this causes an oscillatory motion, since the group velocity is proportional to the derivative of the band structure. The oscillation period $T = 2\pi\hbar/F\,d$ depends on the applied force F and the lattice constant. The resulting amplitude $z_{\mathrm{BO}} = \Delta/2|F|$ is given by the width of the first band Δ and the force. Since this amplitude is only a few micrometres for typical experimental parameters, the Bloch oscillations are conveniently analysed in momentum space via time-of-flight (TOF) absorption imaging.

While the oscillation can be described in a simple 1D model, the complex dynamics in a disordered potential gradient and the role of interactions have to be analysed with a full 3D model. All numerical simulations presented in this work are obtained using the 3D GPE

$$\left[-\frac{\hbar^2}{2m}\nabla^2 + V_L(z) + V_{\mathrm{MF}}(\mathbf{r}) + V_{\mathrm{grad}}(z) + g\,|\Psi(\mathbf{r})|^2\right]\Psi(\mathbf{r}) = \mu\Psi(\mathbf{r}). \tag{2}$$

The cylindrically symmetric magnetic trapping potential is $V_{\mathrm{MF}}(\mathbf{r}) = \frac{1}{2}m\,\omega_\rho^2\,\rho^2 + \frac{1}{2}m\,\omega_z^2 z^2$ with trapping frequencies ω_ρ and ω_z. The optical potential is $V_L(z) = s\,E_{\mathrm{r}}\cos^2(k\,z)$, where s is the lattice depth in units of the recoil energy $E_{\mathrm{r}} = \hbar^2k^2/2m$ and $k = 2\pi/\lambda$ is the wavevector of the optical lattice. The additional homogeneous gradient potential is given by $V_{\mathrm{grad}}(z) = F\,z$.

Due to interactions between the atoms, Bloch oscillations of BECs suffer, in contrast to the case of fermions [12], from dynamical instabilities [29, 30]. In the outer half of the Brillouin zone the nonlinear coupling leads to an exponential growth of small perturbations. Independent of inhomogeneities in the potential they are responsible for a damping of the Bloch oscillations. Therefore, it is necessary to reduce the dynamical instability in order to investigate the effect of the disorder on the Bloch oscillations. This can be accomplished with a combination of a high potential gradient [31] and a reduction of the nonlinear interactions. In a recent work, long-lived

Bloch oscillations of BECs were realized [13, 15] by decreasing the s-wave scattering length with a Feshbach resonance, essentially turning off the atomic interaction. In the experiments reported here the interactions were reduced by decreasing the density of the BEC, to enable the observations of disorder-induced damping of Bloch oscillations.

3. Experimental realization

The experiments were performed with ^{87}Rb BECs in the $F = 2$, $m_F = 2$ state. A detailed description of our apparatus is given in [32]. Nearly pure BECs of up to $N = 3 \times 10^5$ atoms are produced, however all experiments described here were carried out with $N = 5 \times 10^4$ atoms to reduce the interaction energy, and to ensure that no significant thermal background is present. After production of the BEC the magnetic offset field was adiabatically increased to 91 G within 440 ms, thus lowering the radial trapping frequency to $\omega_\perp = 2\pi \cdot 29$ Hz. This reduces the interaction energy by a factor of 6.25, which in combination with low atom numbers sufficiently inhibits the dynamical instability, such that up to four undamped Bloch oscillation periods can be observed. The following procedure was used to observe the Bloch oscillations. After decreasing the radial trapping frequency the intensity of the optical lattice was adiabatically increased to its final value within 60 ms. Subsequently, the atoms were subjected to either a homogeneous potential gradient or a spatially inhomogeneous one for a variable time. Finally all potentials were turned off at the same time and the atomic cloud was detected after a TOF of 30 ms by absorption imaging.

The 1D optical lattice is provided by a standing light field at a wavelength of 825 nm, which is superimposed on the axial direction of the magnetic trap with a waist of $\omega_0 = 140\,\mu$m at the position of the atoms. The investigations were performed at a lattice depth of $2\,E_r$, since low lattice depths lead to a large width of the energy band and therefore to a high maximal group velocity. This results in an oscillation amplitude of the centre-of-mass motion of 80 μm after a TOF of 30 ms, which can be easily detected, while the Bloch oscillations are not affected by the Landau–Zener tunnelling [33].

The homogeneous potential gradient is provided by magnetic coils in anti-Helmholtz configuration, which produce gradients of up to 3.7 G cm^{-1}. This corresponds to an acceleration of 2.4 m s^{-2}.

The inhomogeneity is realized by a disordered optical dipole potential, generated by imaging a randomly structured chrome substrate radially onto the BEC, as described in a previous publication [2]. The correlation length of the disorder is 8 μm and its depth was varied between 0 and $135 \times 10^{-3}\,E_r$, where the depth is defined as twice the standard deviation analogue to [17].

Figure 1 shows absorption images of BECs undergoing Bloch oscillations after 30 ms TOF for a lattice depth of $2\,E_r$ without disorder. One clearly recognizes the oscillation as a motion of the central peak and the periodic appearance of a second peak replacing the main one during an oscillation cycle. Figure 2 shows the centre-of-mass oscillation as well as a theoretical prediction based on a band structure calculation without free parameters. The position of the BEC z_{BO} was calculated by numerically summing the weighted axial positions $z_{BO} = \sum_z \frac{N(z)}{N_{total}} z$. The measured Bloch period was 4.5 ms and the oscillation amplitude was 73 μm which is in good agreement with the theoretical calculations of 4.66 ms and 80 μm for an acceleration of 2.4 m s^{-2} and a lattice depth of $2\,E_r$.

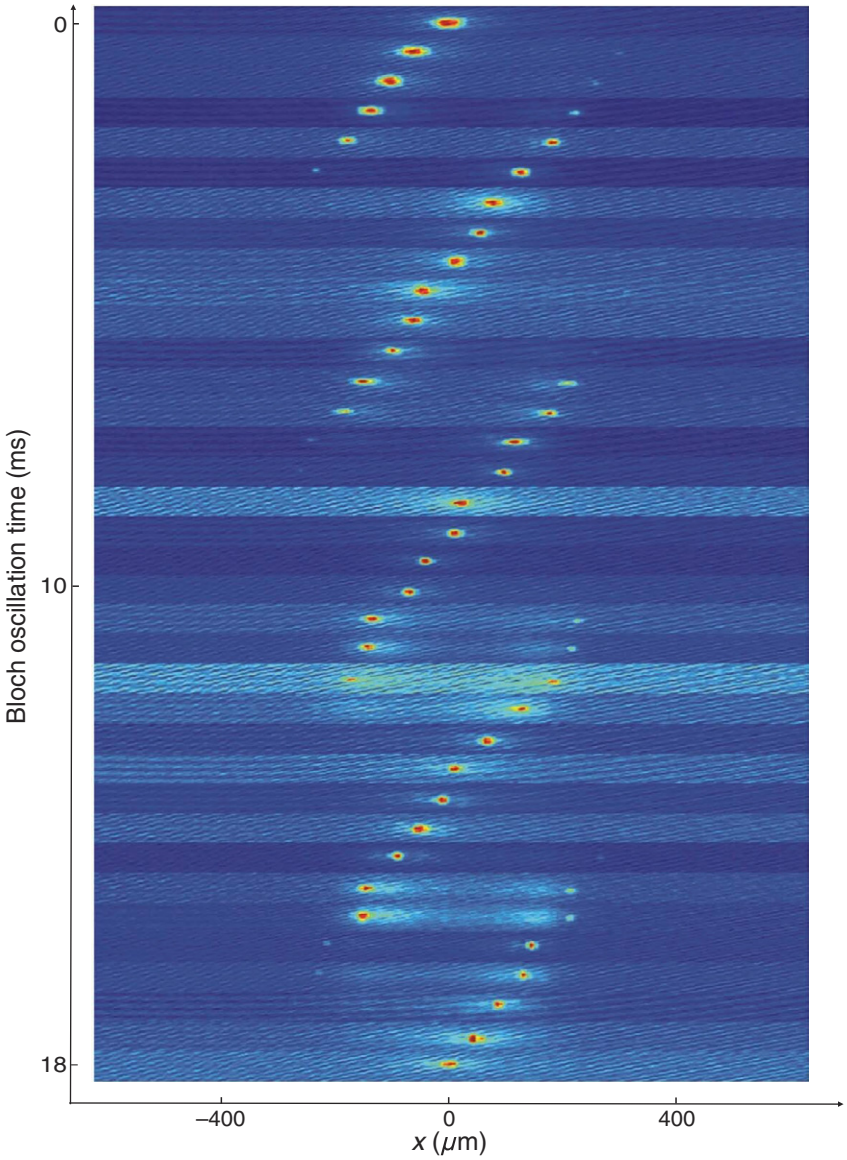

Figure 1. Absorption images after a TOF of 30 ms, for varying Bloch oscillation times. The lattice depth was 2 E_r and the acceleration 2.4 m s^{-2}.

4. Damped Bloch oscillations

The theory of disorder-induced damping of Bloch oscillations was investigated in detail in a previous publication [27] and we only briefly review the important features for the interpretation of the experimental results.

For the analysis of Bloch oscillations in an inhomogeneous potential gradient the GPE (equation (2)) has to be modified by expanding the acceleration term to

$$V_{\mathrm{grad}} = F\,z + V_{\mathrm{dis}}(z), \tag{3}$$

where $V_{\mathrm{dis}}(z)$ denotes the additional optical potential which constitutes the disorder.

Figure 3 shows the centre-of-mass position obtained from numerical simulations of damped Bloch oscillations for a typical disordered potential used in the experiment. One clearly

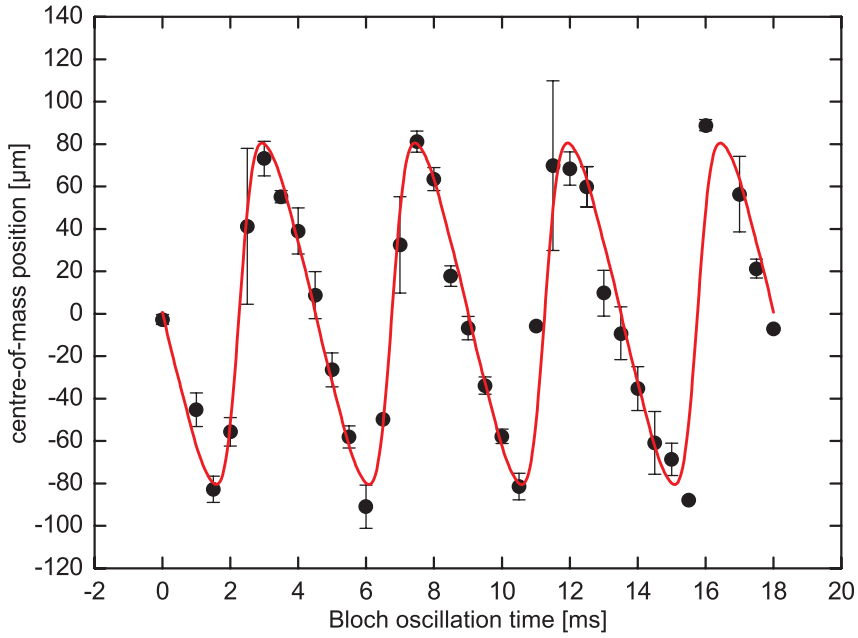

Figure 2. Centre-of-mass position of BECs after a TOF of 30 ms, as a function of the Bloch oscillation time. The parameters are identical to figure 1.

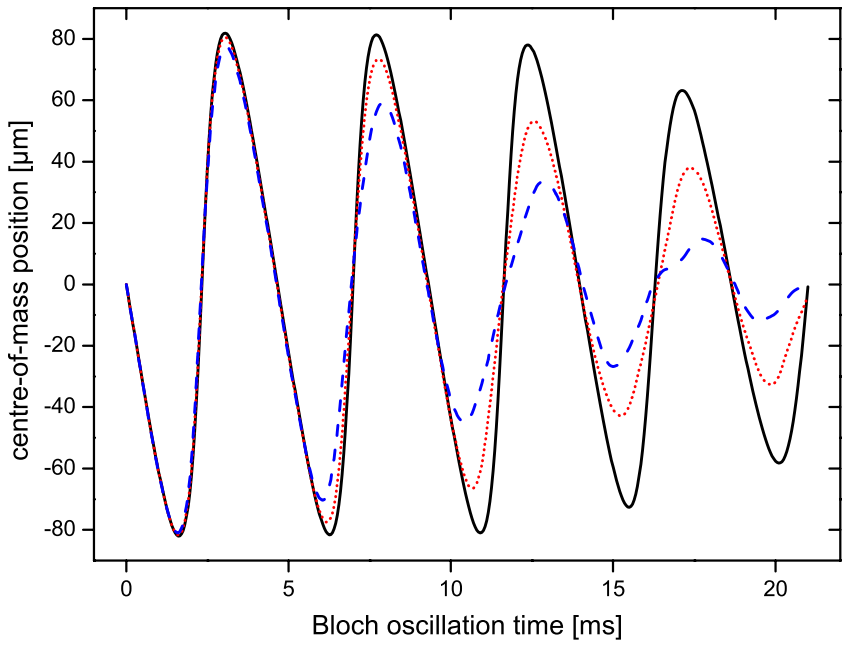

Figure 3. Centre-of-mass oscillation position of a BEC for a lattice depth of 2 E_r, an acceleration of 2.4 m s^{-2} and disorder depths of 0 E_r (black, solid line), 70×10^{-3} E_r (red, dotted line) and 130×10^{-3} E_r (blue, dashed line), obtained from a numerical solution of the GPE.

recognizes that the damping of the oscillations strongly depends on the disorder depth. The damping can be understood qualitatively in terms of the evolution of the phase difference from site-to-site. For an undisturbed homogeneous potential gradient it develops in time according to

$$\Delta\phi(t) = \frac{\delta E}{\hbar}\, t, \tag{4}$$

where δE is the energy offset and $\Delta\phi$ the time-dependent phase difference between neighbouring sites.

The disorder gives rise to a spatially varying energy difference from site-to-site $\delta E(z)$. Therefore, the phase evolution and the quasimomentum vary across the lattice. This broadening of the quasimomentum spectrum causes the damping of the Bloch oscillations, since each q corresponds to one group velocity.

Figure 4 shows the experimental observation of disorder-induced damping of Bloch oscillations for various disorder depths. Note that the lattice depth and the acceleration are identical to the undamped oscillation in figure 2. The graph clearly shows the distinct reduction of the oscillation amplitude for increased disorder. The solid lines are a fit to the data, with the damping coefficient and the periodicity as free parameters. We generate the fit function for the damped Bloch oscillation $z_{\mathrm{DBO}}(t)$ by multiplying the time evolution of the undamped oscillation $z_{\mathrm{BO}}(t)$, obtained from the band structure calculation, with a Gaussian envelope

$$z_{\mathrm{DBO}}(t) = A_0\, \mathrm{e}^{-t^2/\sigma^2}\, z_{\mathrm{BO}}(t). \tag{5}$$

The shape of the envelope is a consequence of the broadening of the quasimomentum distribution in time. The width of this distribution determines the oscillation amplitude, which is reduced compared to the single particle picture, because separate parts of the ensemble simultaneously undergo different phases of the oscillation. Based on the assumption that the width of this distribution increases linearly in time, a Gaussian envelope of the damping amplitude is expected [34, 35].

To quantitatively compare the experimental data to the numerical solutions of the GPE, we show the resulting damping coefficients as a function of the disorder depth in figure 5. The parameters of the simulations correspond to the experimental ones for a typical realization of the disordered potential. Since the damping rate strongly depends on the depth of the disorder potential, the horizontal error bars represent an experimental uncertainty in this depth of 25%. This was estimated by evaluating the depth of the used disorder potential at different positions, while small deviations between the exact shape of the disorder potential in the experiment and in the numerical simulation were not accounted for. The shaded area corresponds to an uncertainty in the atom number of 30%, accounted for in the simulations. Within this uncertainty, we observe good agreement between experimental and theoretical values of the damping coefficients.

To show that the broadening of the quasimomentum spectrum is the underlying mechanism of the damping, we analyse the experimental data with a second approach. Since the dephasing of the quasimomenta increases the number of atoms with varying momenta, the number of atoms in the BEC peaks is reduced [31]. This picture is confirmed by figure 6, which shows numerical results for the time evolution of the momentum spectrum in the presence of a disordered potential gradient. The disorder-induced dephasing leads to an increased blurring of the sharp momentum distribution, as the quasimomenta undergo a non-uniform evolution.

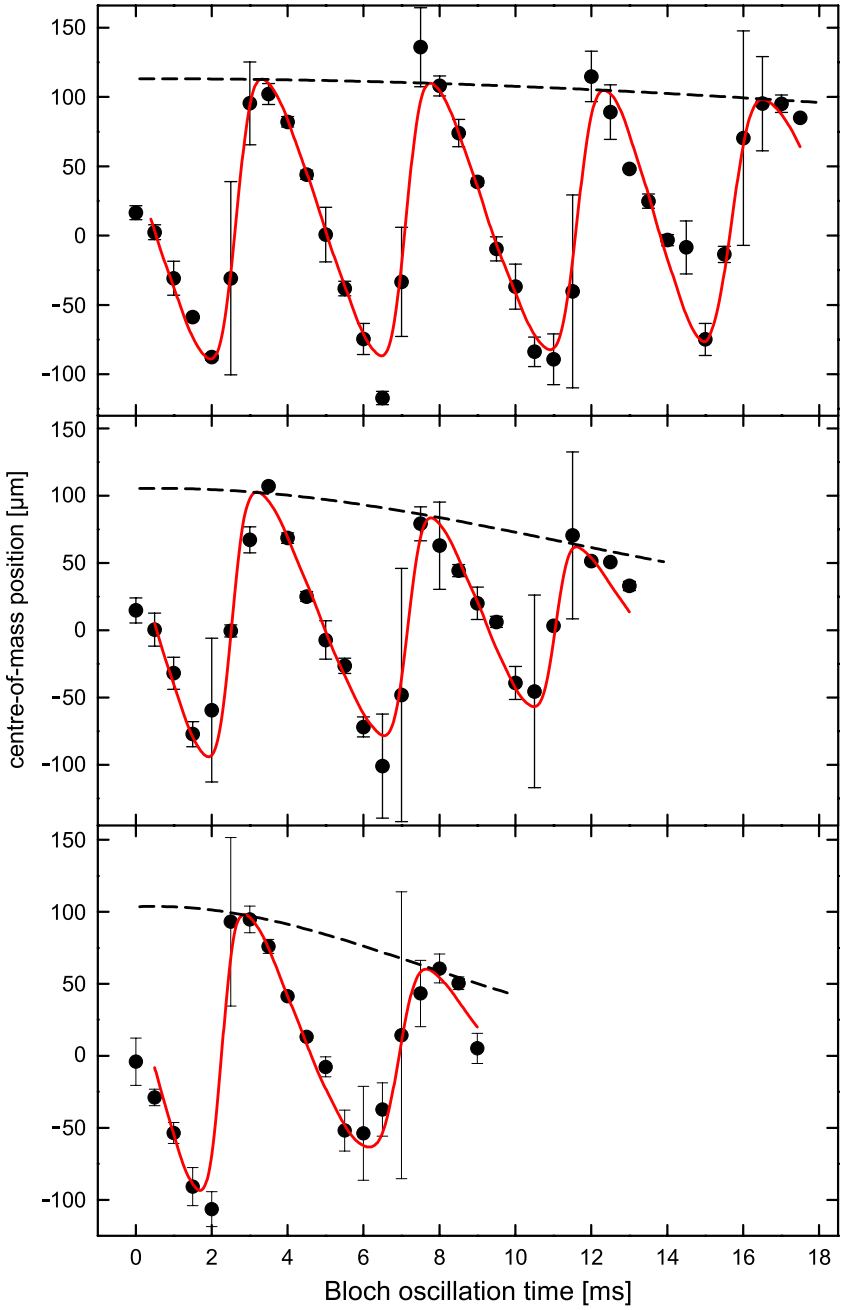

Figure 4. Centre-of-mass position of BECs performing damped Bloch oscillations. The disorder depths were 35, 105 and $135 \times 10^{-3}\, E_r$, from top down. A fit to the data (solid red line) and the Gaussian envelope (dashed black line) due to the damping are also shown. Note that the recorded oscillation time is reduced for increased disorder depth since the broadening of the quasimomentum spectrum causes a strong reduction of the contrast (see figure 8). This significantly reduces the signal-to-noise ratio of the absorption images.

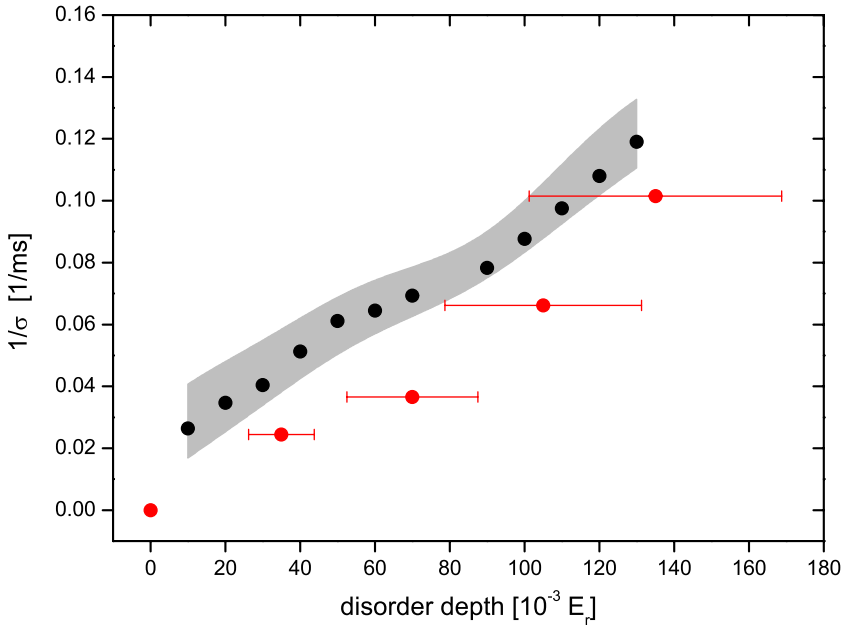

Figure 5. Damping coefficient $1/\sigma$ of the centre-of-mass oscillation in the disordered lattice potential. The damping coefficients were obtained by applying the same fit procedure to the experimental data of figure 4 and the results of the numerical simulations. The red dots represent the experimental data and the black dots the simulations. Similar to the experimental case, the number of Bloch oscillation periods used in the fits to the simulations were reduced for increasing disorder depth. The shaded area corresponds to atom numbers used in the simulations ranging from 3.5×10^4 to 6.5×10^4.

This behaviour is consistent with the absorption images shown in figure 7. In the undisturbed case, sharp BEC peaks are visible whereas the disordered case exhibits a clearly discernible background and a broadening of the peaks due to the dephased quasimomenta.

To analyse this effect quantitatively, we estimate the number of atoms in the BEC N_{BEC} at different times of the Bloch oscillation by fitting Thomas–Fermi profiles to the characteristic peaks of the BEC. The fraction of atoms in the BEC is calculated by comparing the number of atoms in these peaks with the total atom number $N_{\mathrm{frac}} = N_{\mathrm{BEC}}/N_{\mathrm{total}}$.

Figure 8 shows this fraction as a function of the Bloch oscillation time for various depths of the disorder potential. The lines are fits to the data with an exponential decay. A clear reduction in the occupation of the BEC peaks during the evolution of the Bloch oscillation is visible. In all cases the dephasing of the quasimomenta precedes the onset of the damping shown in figure 4. This is in agreement with a Gaussian shape of the damping envelope given in equation (5) and confirms that the dephasing of the quasimomenta is the underlying mechanism for the damping of the centre-of-mass motion. Hence, only a significant broadening of the quasimomentum leads to a relevant damping.

Note that even at a disorder depth of $0E_{\mathrm{r}}$ a reduction and therefore a dephasing is observed due to the interparticle interactions, while the centre-of-mass oscillation in figure 4 is still unaffected.

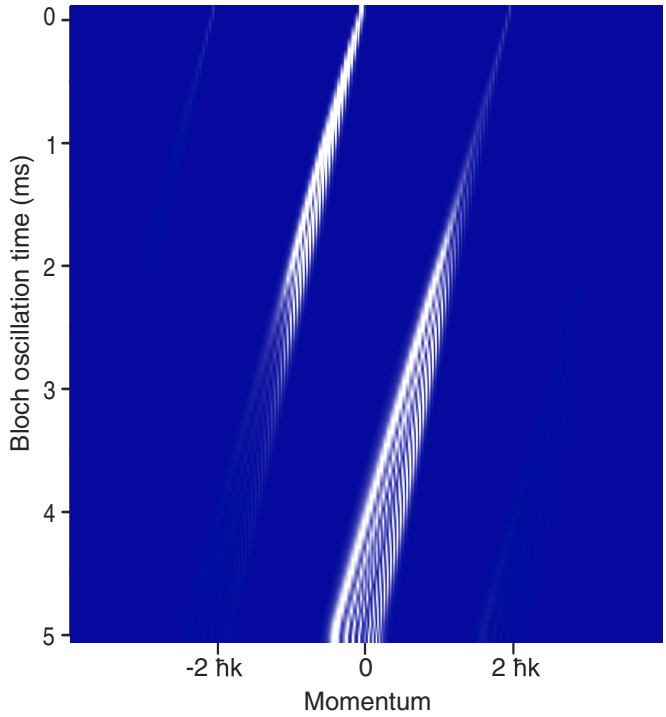

Figure 6. Grey scale plot of the evolution of the momentum distribution during a Bloch oscillation for a disorder depth of $105 \times 10^{-3} E_r$. The lattice depth and the acceleration were identical to the case of figure 3.

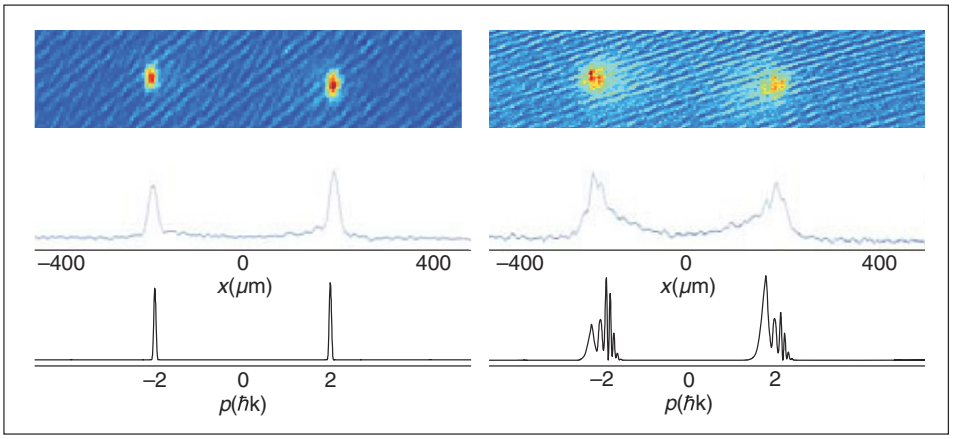

Figure 7. Absorption images of BECs for an oscillation time of 0.5 Bloch periods at an acceleration of $2.4\,\mathrm{m\,s^{-2}}$ and a lattice depth of $2\,E_r$ after a TOF of 30 ms. The left column shows the case without added disorder, whereas the right column corresponds to a disorder depth of $105 \times 10^{-3}\,E_r$. The top row shows the absorption images, the middle row corresponds to the associated axial density profiles and the bottom row contains the momentum spectrum obtained from our simulation.

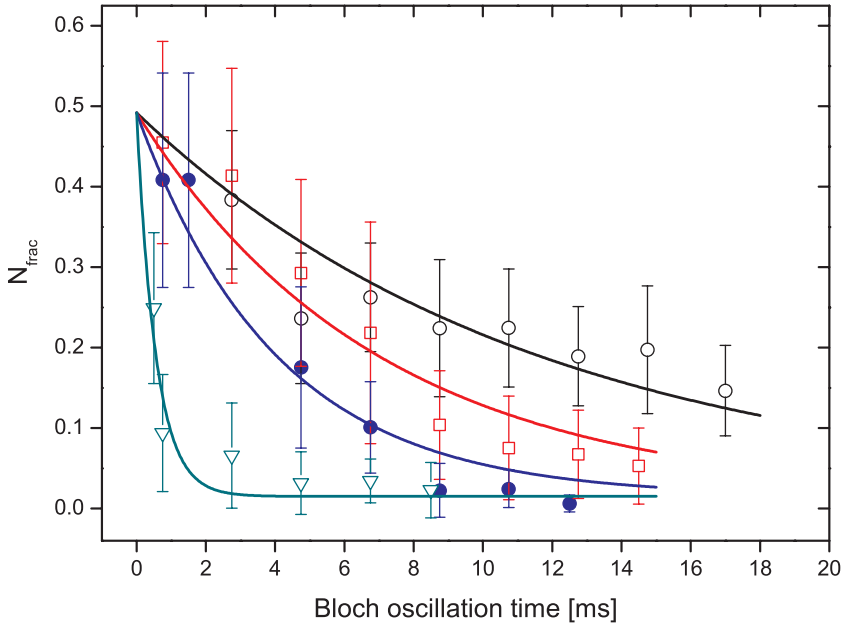

Figure 8. Fraction of atoms in the BEC after a TOF of 30 ms as a function of the Bloch oscillation time. Shown are four depths of the disorder potential of $0E_r$ (black circles), $35 \times 10^{-3} E_r$ (red squares) $70 \times 10^{-3}\, E_r$ (blue dots) and $135 \times 10^{-3}\, E_r$ (green triangles). The curves correspond to a fit with an exponential decay. Residual imaging effects (see figure 7) result in an overestimate of the total number of atoms. Therefore N_{frac} is 0.5 even for pure BEC without any discernible thermal fraction.

The decay times τ from figure 8 are shown in figure 9 as a function of the disorder depth. The decreasing fraction of atoms in the BEC peaks again confirms that stronger disorder leads to faster dephasing of the momentum distribution and that this broadening of the quasimomentum is the underlying mechanism for the damping of the Bloch oscillations.

5. Conclusion

We have presented the first experimental investigation on disorder-induced damping of Bloch oscillations of BECs. The application of an additional disorder potential during the oscillation leads to a strong damping of the centre-of-mass motion and to a significant reduction of the fraction of atoms in the BEC. The observed damping rates are in good agreement with predictions based on numerical solutions of the full GPE and show that the underlying physical mechanism for the damping is the broadening of the quasimomentum spectrum due to the spatially varying phase evolution of the condensate.

We show that even a very small disorder results in fast dephasing of the quasimomentum and therefore damping of the Bloch oscillation. Since the disorder presented here is equivalent to a spatially inhomogeneous force, the results are of special interest for the application of Bloch oscillations for high precision spectroscopy of very small forces. To reach high precision in such experiments it is essential to follow a large number of Bloch oscillations. This number may be reduced if the observed force is spatially inhomogeneous on length scales comparable

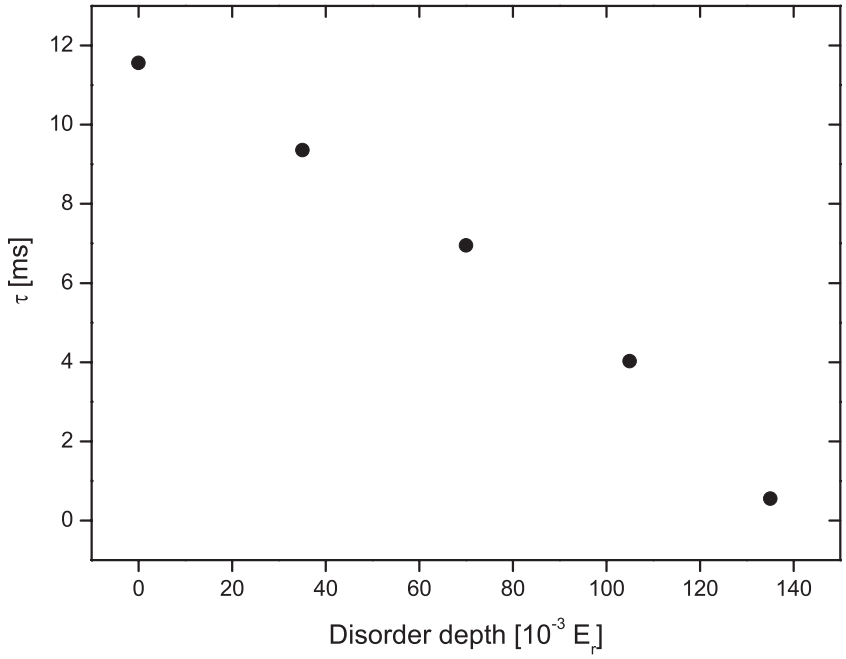

Figure 9. The decay times τ of figure 8 are shown as a function of the disorder depth. Strong reduction is observed even for moderate disorder depths.

to the extent of the condensate. The good agreement between theory and experiment shows the applicability of our method to analyse the effects of spatially varying forces, and allows for estimates of the effect of small inhomogeneities for future experiments.

Acknowledgments

We thank M Lewenstein for fruitful discussions. This work was supported by the Centre for Quantum Engineering and Space-Time Research and by the Deutsche Forschungsgemeinschaft within the SFB 407, the SPP1116 and within the European Graduate College Interference and Quantum Applications.

References

[1] Damski B *et al* 2003 *Phys. Rev. Lett.* **91** 080403
[2] Schulte T *et al* 2005 *Phys. Rev. Lett.* **95** 170411
[3] Sanchez-Palencia L *et al* 2007 *Phys. Rev. Lett.* **98** 210401
[4] Lugan P *et al* 2007 *Phys. Rev. Lett.* **99** 180402
[5] Fallani L *et al* 2007 *Phys. Rev. Lett.* **98** 130404
[6] Greiner M *et al* 2002 *Nature* **415** S39
[7] Bloch F 1928 *Z. Phys.* **52** 555
Zener C 1934 *Proc. R. Soc. Lond.* A **145** 523
[8] Ben Dahan M *et al* 1996 *Phys. Rev. Lett.* **76** 4508
[9] Wilkinson S R *et al* 1996 *Phys. Rev. Lett.* **76** 4512
[10] Morsch O *et al* 2001 *Phys. Rev. Lett.* **87** 140402

[11] Waschke C *et al* 1993 *Phys. Rev. Lett.* **70** 3319
[12] Roati G *et al* 2004 *Phys. Rev. Lett.* **92** 230402
[13] Fattori M *et al* 2008 *Phys. Rev. Lett.* **100** 080405
[14] Ferrari G *et al* 2006 *Phys. Rev. Lett.* **97** 060402
[15] Gustavsson M *et al* 2008 *Phys. Rev. Lett.* **100** 080404
[16] Lye J E *et al* 2007 *Phys. Rev.* A **75** 061603
[17] Lye J E *et al* 2005 *Phys. Rev. Lett.* **95** 070401
[18] Clément D *et al* 2005 *Phys. Rev. Lett.* **95** 170409
Fort C *et al* 2005 *Phys. Rev. Lett.* **95** 170410
[19] Chen Y P *et al* 2008 *Phys. Rev.* A **77** 033632
[20] Horak P, Courtois J-Y and Grynberg G 1998 *Phys. Rev.* A **58** 3953
[21] Diener R B *et al* 2001 *Phys. Rev* A **64** 033416
[22] Gavish U and Castin Y 2005 *Phys. Rev. Lett.* **95** 020401
[23] Ospelkaus S *et al* 2006 *Phys. Rev. Lett.* **96** 180403
[24] Folman R *et al* 2002 *Adv. At. Mol. Opt. Phys.* **48** 263
Henkel C, Kruger P, Folman R and Schmiedmayer J 2003 *Appl. Phys.* B **76** 173
Wang D-W, Lukin M D and Demler E 2004 *Phys. Rev. Lett.* **92** 076802
[25] Cladé P *et al* 2006 *Phys. Rev. Lett.* **96** 033001
[26] Carusotto I *et al* 2005 *Phys. Rev. Lett.* **95** 093202
[27] Schulte T *et al* 2008 *Phys. Rev.* A **77** 023610
[28] Cristiani M *et al* 2002 *Phys. Rev* A **65** 063612
[29] Menotti C, Smerzi A and Trombettoni A 2003 *New J. Phys.* **5** 112
[30] Modugno M, Tozzo C and Dalfovo F 2004 *Phys. Rev.* A **70** 043625
[31] Cristiani M *et al* 2004 *Opt. Express* **12** 4–10
[32] Cacciapuoti L *et al* 2003 *Phys. Rev.* A **68** 053612
[33] Zener G 1932 *Proc. R. Soc. Lond.* A **137** 696
[34] Witthaut D, Werder M, Mossmann S and Korsch H J 2005 *Phys. Rev.* E **71** 036625
[35] Hartmann T, Keck F, Korsch H J and Mossmann S 2004 *New J. Phys.* **6** 2
[36] Guidoni L, Triché C, Verkerk P and Grynberg G 1997 *Phys. Rev. Lett.* **79** 3363
Grynberg G, Horak P and Mennerat-Robilliard C 2000 *Europhys. Lett.* **49** 424